DESIGN OF A HIGH-SAMPLING-RATE FORCE MEASUREMENT SYSTEM FOR A HYPERSONIC WIND TUNNEL

Asa Guldbrandsen **Maxwell Gjevre** **Alexander Lee** **Luke Herter** **Miles Owens**

ABSTRACT

Hypersonic flow (a classification given to flows above Mach five) is studied to better understand the flight conditions for experimental aircraft, re-entry vehicles, advanced missiles, and minor astronomical bodies. The use of pulsed lasers in hypersonic flow environments is an emerging field of research that is applicable to defense, high speed travel, and astronomy. This project aims to design, build, and test a data collection system for a group at the Laboratory for Laser Energetics (LLE) that can characterize a shock wave produced by a pulsed laser acting on a body in hypersonic flow. Pulsed lasers operate on the nanosecond timescale (6 ns pulse length), and most hypersonic test facilities can deliver steady state flow on the millisecond timescale (<100 ms), depending on the desired flow conditions. These conditions create the need for high sampling rate data acquisition and carefully calibrated mechanical systems. The Hyper group investigated the use of a custom-built fiberoptic interferometer, rosette strain gauges, and schlieren imaging for collecting data from a test subject in hypersonic flow. Through the testing of two distinct prototypes, the group was able to develop a better understanding of design constraints imposed by hypersonic flow and the behavior of pulsed laser while also working towards a better characterization of the capabilities of strain gauges and interferometric systems in measuring these extreme conditions. The use of strain gauges, fiber-interferometry, and photon doppler velocimetry (PDV) could be used in a third iteration sting that collects impulse data from pulsed lasers in hypersonic flow.

PROBLEM DEFINITION

The LLE is studying the interactions of lasers with objects in hypersonic flow. Currently, the lab does not have a method of directly laser applied force. Commercially available load cells do not have an appropriate combination of sample rate and resolution required to measure such a short, intense deposition of energy in the extreme conditions presented by hypersonic flow. This project aimed to deliver a prototype measurement device capable of collecting data on the shock produced by a pulsed laser in a hypersonic wind tunnel. Such a device would additionally enable the correlation of analytical predictions of laser applied force and measured applied force. At its core, this project aimed to develop a better understanding of different measurement techniques and their applicability to measuring pulsed laser effects in hypersonic flow. Due to the widespread use and availability of strain gauges, a better understanding of their ability to resolve pulsed laser shock was desired. Finally, the group sought to experiment with creating a fiber interferometer as its resolution and sampling rate is very high.

REQUIREMENTS, SPECIFICATIONS, DELIVERABLES

The main deliverable for this project was a prototype device designed to measure forces applied by a laser in at least one degree of freedom. In addition to the prototype, the team was tasked with providing simulation data, analysis data, and other supporting documentation for the prototype. Included in the documentation was a technical report outlining the design of the system and progression between iterations. The provided documentation, prototype, impulse hammer, and measurement system would allow for recreation of the device and a clear path forward for future work and redesign.

TABLE 1
REVISED SPECIFICATIONS

	Value	Specification
1	10 FoS	Minimum factor of safety for mount
2	1 DoF	Minimum data collection axis
3	300 kS/s	Minimum sampling rate
4	0.2 lb_f	Minimum resolved load from impulse hammer
5	500 lb_f	Minimum acceptable flow load
6	1 ft^3	Maximum design envelope
7	48 in	Maximum flow diameter
8	1 kHz	Minimum natural frequency

TABLE 2
REVISED REQUIREMENTS

	Requirement
1	Must not experience mechanical failure when subjected to hypersonic flow
2	Must be compatible with the diagnostics known to the group
3	Must be able to resolve impulse load applied via pulsed laser

The requirements and specifications that governed the design of the apparatus can be found in Table 1,2. Throughout the project, these requirements and specifications were modified to more accurately characterize hypersonic flow and pulsed laser effects.

The initial requirements and specifications, Table A1, represented the initial understanding of pulsed laser effects. Upon further testing and research, the team determined that revised requirements and specifications, Table 1,2, were required.

The first requirement stated that the prototype must not mechanically fail when subject to hypersonic flow. Mechanical failure was defined as any permanent deformation in any of the components. This requirement was created to ensure repeatability during testing and ensure that the apparatus would not damage the hypersonic test facility. The second requirement stated that the prototype must make use of measurement tools used by the group at the LLE. These known diagnostic tools were determined to be interferometry, strain gauges, and Schlieren imaging. This requirement was created to ensure that the prototype could easily be used in the future. The third requirement stated that the system must be able to detect and resolve an impulse load delivered by a 2.2 Joule pulsed laser applied in a lab setting, outside of hypersonic flow. This requirement was implemented in the revised requirements and specifications after the researchers found that this task was much harder than expected. This requirement was created to ensure that the prototype would repeatably and accurately characterize pulsed laser effects.

The first specification stated that all mount elements would be designed with a factor of safety of 10. This specification primarily influenced the choice of hardware and mounting geometry. This specification would ensure the satisfactory result of the first requirement. The second specification stated that data from the pulsed laser would be collected in at least one degree. This specification was created to ensure that the laser pulse, when applied orthogonally to the flow direction, could be accurately measured and characterized using the prototype. The third specification stated that a minimum sampling rate of 300 kS/s would be sufficient for data collection. This specification was based on estimates of the timescale of the pulsed laser shock and commercially available data acquisition systems. This specification would ensure that the full response of the prototype could be analyzed and no data would be lost due to the instantaneous nature of the event. The fourth specification stated that the prototype should be able to resolve a minimum load of 0.2 lb_f applied via an impulse hammer. This specification was based on the researchers' understanding of the pulsed laser being studied. This specification was originally defined as a maximum load of 2000 lb_f applied as an impulse load. It was found that a minimum resolution more accurately governs the design of the prototype. This specification is closely tied to the third requirement. The fifth specification stated that the prototype should be designed to withstand at least 500 lb_f applied in the direction of hypersonic flow. This specification was based on the researchers' understanding of hypersonic flow and calculations of expected pressure on the wedge. This specification is closely related to the first requirement. Specification five was originally set to a maximum force value of 5000 lb_f which was determined to result in an over designed prototype. Specification six stated that the prototype must be contained within a maximum build envelope of a 1 by 1 by 1 ft cube. This envelope was determined based on the wind tunnel utilized for current laser-flow interaction studies at CUBRC[1]. Specification seven stated that the prototype must exist within a flow diameter of 48 in. This specification was created to ensure that the prototype would fit in the CUBRC wind tunnel and as long as the prototype is not close to the 48 in diameter, it would stay outside of the boundary layer. The eighth specification stated that the prototype should be designed to have a minimum natural frequency of 1 kHz. This specification was created to ensure that during testing, the prototype would not vibrate to the point of failure. The 1 kHz value was influenced by the capabilities of NX simulations and the researchers' knowledge of vibrational effects in hypersonic flow. In the initial specification set, the group highlighted the importance of temperature effects on the accuracy of interferometric data collection. This specification stated that a minimum 10 °C temperature change must not result in adverse effects in the mechanical or measurement system. This temperature change was based on the expected change in temperature due to hypersonic flow delivered by the CUBRC wind tunnel. This specification was cut from the final specification set due to the removal of an interferometric measurement system in the final design.

CONCEPTS

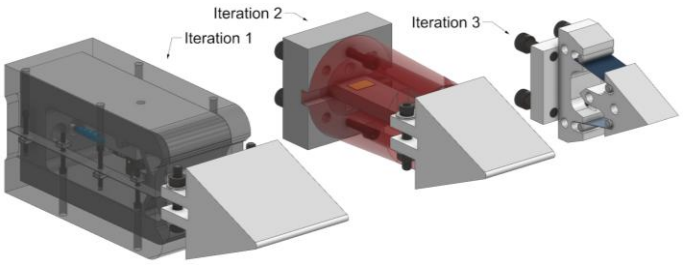

Figure 1: Iteration one, two, and three side by side. Iteration one and two were manufactured.

Over the course of the project's development, the Hyper group switched between various designs. The work breakdown structure in Table A1 and Figure A1 describes the project path outline. The first step in problem definition was to develop an understanding of how a hypersonic wind tunnel works, Figure A2. Based on background research, the team found that hypersonic wind tunnels make use of high-pressure driving gas and an ambient pressure driven gas which are combined and released into a vacuum chamber. This creates hypersonic flow around the sample. The first sting design used strain gauges and

[1] Calspan-University of Buffalo Research Center

a laser displacement sensor from Keyence, which would be placed inside the hypersonic flow Figure A3. This design was ruled out because the laser beam would be exposed to hypersonic flow, which would likely result in inaccuracy in sensing. From there, the team pivoted to using a high-speed camera that could image displacement through hypersonic flow (Schlieren imaging). As well as using an LK-G displacement sensor, which, when combined with a parallel beam, could measure the displacement of the wedge. After talking to a representative from Keyence, the team found that the sensor was not vacuum rated and likely would not work even in a rough vacuum. The system was subsequently redesigned and outfitted with a pressure chamber inside the sting (Figure A4). The issue with this design is that once the sensor was added, it would be impossible to remove it without damaging the system. From there, the sting was redesigned to allow for the wires and measuring devices to be mounted within (Figure A5). After looking into commercially available interferometry systems, it was determined that the lead times were too long for this project. Additionally, creating a custom interferometric system was allowed for a setup tailored for the specific experiment while reducing cost. Although a custom system had its own challenges due to lack of experience and required two group members to conduct research and design the system for over a month. This leads to the iteration one design path. The group decided to use 1018 cold-rolled steel due to the high elastic modulus, and 6061 aluminum failed in the simulation under the load case of 1000 lb_f. 6061 aluminum was chosen for the wedge due to its cost and machinability. For the first iteration, a sting design seen in Figure A6 was implemented. This design iteration made use of shadowgraphy via a phantom camera, strain gauges, and a custom-built interferometer. As shown in Figure A7, strain gauges and collimators could be mounted inside the sting. This first iteration design was further revised to its final form as depicted in Figure A8. The system geometry was designed based on FEM as shown in Figure A9A. This design allowed for known rotation about the point where the webs meet. This rotation would allow for strain measured by strain gauges and tilt measured by the custom-built interferometer.

In addition to the concept selection for the first iteration design, the team had to determine the most effective measurement system to use. The pugh matrix, seen in Table A3, outlines this decision-making process. The Phantom TMX 7510 high-speed camera was chosen, as it has been used to capture pulsed laser ablation data in hypersonic flow in the past. It was concluded that the most effective path forward would pursue the design and manufacturing of a custom-built fiber interferometric system and strain gauges. The plan was for the strain gauges to serve the purpose of a robust data collection system while the interferometer would likely have provided more sensitive and higher resolution data. Using these three systems in parallel would allow the team to better characterize the effects of pulsed lasers in hypersonic flow.

The custom interferometric system employed fiber-optic cables to improve flexibility and ease of use during testing, Figure A14. A helium-neon (HeNe) laser emitting red light at 630 nm was directed into a collimator. To achieve the precise alignment required, the laser was mounted on a tip-tilt stage, while the collimator was positioned on a three-axis translation stage, Figure A15. This combination provided five degrees of freedom, which was necessary because of the extremely small core diameter of the fiber-optic cables. Slight misalignment would prevent the laser light from coupling effectively into the fiber.

Before entering the fiber-optic system, the laser beam was polarized. Polarization refers to the orientation of the electric field oscillations in the light wave. In polarized light, these oscillations are confined to a single plane, which is essential for interferometry because it ensures consistent wave behavior and maximizes interference contrast.

The polarized beam then entered a fiber-optic coupler, which split the incoming light evenly into two paths. One beam was directed toward a stationary reference mirror, while the other was sent to the test specimen. After reflecting from their respective surfaces, both beams reentered their respective fibers and returned to the coupler, where they recombined. The resulting interference pattern, which contains information about any displacement of the test surface, was then routed through a fourth fiber. Finally, this output light was projected onto a Phantom high-speed camera for recording and analysis.

To determine the mechanical response and to optimize the chosen design repeated FEA analyses were done on the chosen concept. The results that were prioritized from this were displacement and strain, since those were the metrics measured by the three planned data collection systems. So, the end goal of the simulations was to determine if the compliant mechanism can withstand the applied force by the laser, calculate maximum strain, determine what material to use, and find expected displacement at the tip.

The FEM model for the compliant mechanism can be seen in Figure A9A. The goal of the study was to find an appropriate thickness for the X-shaped webs such that the mirror face, strain, and tip displacement are in measurable ranges for the planned data collection methods.

The “Frankenstein Model” is seen in Figures A17, A19. These models were 3D printed with PLA and used as proof of concept that a compliant mechanism would work to translate the displacement away from the wedge into a place that is more easily measurable. They were also used to show the group a rough idea of what the iteration one design plan was.

After the initial prototype was developed, Figure 1, the full-scale device was manufactured, Figure A20, and tested. Initial testing revealed that the structure was too stiff to produce measurable displacement under impulse laser loading. This outcome stemmed in part from a misunderstanding regarding the project requirements and loading conditions provided.

As a result, the team pivoted to a simplified cantilever beam and wedge configuration, Figures 1, A10, A21. This redesign was also influenced by time constraints and the failure of a power supply, which eliminated interferometry as a viable data acquisition method. For the revised setup, the applied impulse load was estimated to range from 25 to 100 lb_f over a duration of 1 millisecond.

To determine the appropriate beam thickness, a series of simulations were conducted in Siemens NX. Stress and displacement were evaluated for varying beam thicknesses and load cases, as shown in Table A4 and Figure A22. The maximum stress occurred at the edge of the chamfer, Figure A22, while the maximum displacement was observed at the tip of the wedge. The material of the beam and the mounting device for the cantilever portion were both 1018 cold-rolled steel. This allowed the cantilever portion to be welded directly onto the mount.

Following fabrication and testing of the redesigned device, no noticeable displacement was observed when the structure was subjected to laser loading due to the device being too stiff. This caused the group to pivot again.

Once it was determined that the design was still too stiff, the group changed directions again and conducted a simple test on a 12” by 1” by 1/8” 6061 aluminum beam to see if any displacement could be seen under an impulse laser applied force. From this the team saw an electrical response, but it was unclear if this was due to a displacement or another electrical phenomenon, Figure A23A, A23B. One theory for the cause of this result was that the laser produced a longitudinal wave propagating through the beam, instead of displacing the beam tip. Due to the material properties of this beam, the team expected that any laser impulse at the beam end would result in a large strain reading on the gauge. Given that the expected result was not immediately observed, more research is needed to better understand the response of strain gauges subject to pulsed laser response.

After observing unexpected results, the team shifted its focus to investigating the effects of impulse laser loading on strain gauges. To support this effort, three Wheatstone bridge circuits, shown in Figure A24, were designed and built to amplify the signals generated by the strain gauges mounted on the previously described Al 6061 beam. These circuits were connected to a rosette strain gauge configuration, allowing strain data to be recorded during each laser shot. By conducting multiple tests, the team was able to collect a dataset for analysis. This experimental approach provided the foundation for interpreting unexpected measurements and drawing conclusions about the strain gauges' response to impulse laser loading.

MECHANICAL ANALYSIS

PART I: TOLERANCE

The mechanical interface between the interior slot of the wedge (Drawing seen in Figure A25) and the bill of the bar (Drawing seen in Figure A26) is a location where proper tolerances were relevant. The assembly required the bar’s reduced-section, specified at a thickness of 0.300 in. ± 0.005 in. to be slotted into the Wedge’s machined slot which has a width of 0.30 in + 0.02 in. – 0.00in.

A worst-case stack up analysis revealed a possible dimensional conflict that could prevent a standard clearance fit. Under maximum material conditions (MMC), the wedge slot would be 0.30 inches wide, while the bar’s tongue thickness reached a maximum value of 0.305 inches. This returned a worst-case interference of 0.005 inches.

Given that the bar was fabricated from 1018 Steel and the wedge from 6061 aluminum, an attempt at forced assembly at MMC would result in permanent deformation of the wedge slot. Overall to ensure a functional slip or clearance fit during assembly, the wedge slot dimensions were revised to account for manufacturing variances.

PART II: FATIGUE

In the final compliant mechanism design, there were multiple bolt connections. The back plate which connected the mechanism to the adapter plate, and the adapter plate which connected the back plate to CUBRC’s base sting structure. Focusing on the adapter plate there are four 5/16”-18 bolts attaching it to CUBRC’s structure.

Newton’s Sine-Squared Law:

$$C_p = 2sin^2(\theta) \quad (1)$$

Used to find coefficient of pressure across a surface in flow of Mach>>1, the assumption being that flow particles transfer all momentum to the surface of the wedge

Using a half angle of 22.5 degrees, Newton’s Sin-Squared Law yielded a coefficient of pressure of 0.293. This value was then fed into the pressure equation using a V=7877.3 ft/s and a simulated air density at a height between 10km and 30km yielding air density (ρ) values between 7.9656E-04 slugs/ft^3 to 3.4530E-05 slugs/ft^3.

Coefficient of Pressure to Pressure:

$$P = C_p \frac{1}{2} \rho V^2 \quad (2)$$

Used to calculate pressure on wedge surface

This yielded pressure values of 7241.2 slug/ft*s^2 to 313.9 slug/ft*s^2 respectively. In the proceeding calculations a worst-case scenario was assumed, so 7241.2 slug/ft*s^2 was selected.

Force Calculation:

$$F_t = PA \tag{3}$$

Used to calculate the total force air pressure applies on the wedge surface

The wedge has a total frontal area (A) of 9 in^2 (0.0625 ft^2). This value went into the Force Calculation equation, and it was found that in the worst-case scenario the air flow over the wedge yields a force perpendicular to the surface of the wedge equal to 452.58 lb$_f$. After breaking this into an axial and normal force it was found that the axial load is 173.2 lb$_f$, and due to the wedge being symmetric the normal forces cancel out becoming 0 lb$_f$.

Calculating the torque spec of these 4 5/16"-18 bolts was done by using the bolt torque-preload relation.

$$T = KdF_i \tag{4}$$

Where the preload force is:

$$F_i = 0.75A_tS_p \tag{5}$$

The bolts used were Grade 5 bolts with a proof strength (S_p) of 85000 psi, a tensile stress area (A_t) of 0.052 in^2, a coefficient of friction (K) value of 0.30, and a major diameter (d) of 5/16". This yields a preload of 3315 lb$_f$ and a torque spec of 25.9 ft-lb.

In this case the compressional load of 173.2 lb$_f$ had little to no impact on the torque spec, as the load was distributed meaning that there is only 43.3 lb$_f$ experienced on each bolt. Comparing this to the target preload of 3315 lb$_f$ the load of the air pressure only represents 1.31% of the bolts preload. This load is negligible.

Looking at an expected applied load of 1000 lb$_f$ for 1 millisecond acting 6 inches away from the bolts. This created a bending moment of 6000 in-lb$_f$ for 1 ms. This was transferred to the bolts which are on a 1-inch circle causing each bolt to experience 1500 lb$_f$ of tension or compression. The preload plus this applied load created a worst-case load scenario on the top bolts of 4815 lb$_f$ of tension, but 1815 lb$_f$ of clamping force remained. The minimum tensile strength for a Grade 5 5/16" bolt is 6300 lb$_f$. This means that under the applied load the bolts were found not to fail, and the adapter would not separate from the sting in CUBRC's wind tunnel.

A fatigue analysis on the worst-case load scenario on the top bolts yielded the result that under the Modified Goodman Criterion predicts a finite life. This was found by using ultimate strength (S_{ult}), σ_a, σ_m, and Se. The modification factors for the bolt were found to be Ka=0.6923, K_b=1, K_c=0.85, K_d=1, K_e=0.8139, and K_f=0.33. With a S_{ult} value of 170 ksi S_e was to be 13.43 ksi using the endurance strength equation.

$$S_e = K_aK_bK_cK_dK_eK_f\frac{S_{ult}}{2} \tag{6}$$

Using the maximum tension felt in a bolt F_{max} of 4815 lb$_f$ of tension and the minimum tension F_{min} of 3315 lb$_f$ of preload and the following equations, the stress amplitudes σ_a and σ_m were found to be 14.31 ksi and 45.94 ksi, respectively.

$$\sigma_a = \frac{F_{max} - F_{min}}{2A_t} \tag{7}$$

$$\sigma_m = \frac{F_{max} + F_{min}}{2A_t} \tag{8}$$

Where A_t is the tensile stress area

Then the values of σ_a, σ_m, Se, and Sult were inserted into the Modified Goodman Criterion of:

$$\frac{\sigma_a}{S_e} + \frac{\sigma_m}{S_{ult}} \geq 1 \tag{9}$$

The left side of the equation yields a value of 1.34. As this value is greater than 1 the Modified Goodman Criterion predicts a finite life.

PART III: SIMULATION

Upon selecting the compliant mechanism concept, the next task was to use simulation tools, such as NX NASTRAN, to determine the exact geometry and material that will exhibit the desired behavior. Based on the predicted sensitivity of the interferometry system, the team targeted a mirror tilt of 0.1 degrees when loaded by 1000 lb$_f$ for 1 millisecond. The exact spatial and temporal distribution for the load case can be seen in Figure A28. The primary independent variable which was used to adjust maximum stress and mirror tilt was the thickness of the webbing in the compliant mechanism.

The FEM model can be seen in Figure A9A. A 2" thick paver CQUAD4 mesh was applied to a two-dimensional profile of the compliant mechanism with an element size of 0.05" within the main body and a reduced element size of 0.0025" at points of interest. A convergence study was done on this refinement sizing and can be seen in Figure A9B. This meshing strategy was selected to reduce the computational power spent on regions that experience little stress and increase the fidelity in regions that have stress concentrations, such as the joint of the webbing and the diving board. The model has a fixed constraint along the rear face and uses the load case described above. SOL129 with a time step of 1 microsecond was used to study the nonlinear transient response of the body. In deciding what material to make the mechanism from, the maximum stress was the first thing

considered. The FEA found that there is a max stress of 44.25 ksi at the fillet connecting the compliant mechanism to the wedge connector, as seen in Figure A12. This value exceeds the yield stress for 6061 Aluminum, so 1018 HR Steel was considered next. 1018 HR Steel has a yield strength of 50 ksi, which results in a Factor of Safety of 1.13. Since steel is significantly stiffer than aluminum, we used the FEA results to ensure that the mirror tilt was still in the acceptable range. The simulation showed that the mirror would tilt by 0.09 As this meets the material demands, is easily procurable, and can be easily manufactured. The team selected 1018 steel for the main body of the device.

After the team pivoted to a cantilever-based mechanism, another FEA study was conducted to determine dimensions for a steel beam that will exhibit the desired response. The primary independent variable for this study was beam thickness. To examine the theoretical resolution of each setup, simulations were done across a range of scale factors applied to the same temporal load distribution as before, seen in Figure A28A. The scale factors tested were 24.5, 25, 50, and 100. The results of this study can be seen in Table A4, and the team used this information to select a 0.3" thick 1018 steel beam.

The third iteration, the spring steel flexure design, also needed simulation work done. The team was interested in sizing the plates to tune the buckling response of the setup. If the plate structure buckled, it would no longer exhibit the predictable "four-bar" kinematic behavior intended. By applying a 0.0033" thick shell mesh to the plate geometry and representing the wedge with RBE2 elements, the simulation results below were obtained through NASTRAN SOL105.

TABLE 3
BUCKLING ANALYSIS

1st Eigenvalue		Plate Length (in.)		
		2	2.25	2.5
Half-Angle (deg.)	10	1.73	1.41	1.18
	15	1.92	1.57	1.31
	20	2.03	1.65	1.37
	25	2.07	1.68	1.38
	30	2.06	1.65	1.36

MANUFACTURING

The manufacturing methods employed during the development of this project varied greatly depending on the use of the parts. However, as a high-level overview, the vast majority of both full iterations of the sting, and of the to-be-built 3rd iteration sting needed to be manufactured out of materials such as 6061 aluminum or 1018 steel for their high elastic modulus, high machinability, and weldability (for steel). However, additive manufacturing was also leveraged for non-load bearing components that could be made from comparatively low-strength thermoplastics like PLA and ABS.

The first major component in the first iteration of the sting that needed to be manufactured was the compliant mechanism itself. This component was the single most complicated part that the team designed throughout the development of the project. The elected material for this component was 1018 steel after analysis with the current load cases was completed. Its design was mostly governed by the planned manufacturing technique: wire electrical discharge machining (EDM). Most features of this part could be performed with only a couple of operations on a wire EDM machine. Additionally, because the part was thicker than 1 inch and had features such as internal sharp corners, more traditional manufacturing methods like CNC machining could not be easily utilized for the majority of the part's features. Because the University of Rochester does not have the capabilities to manufacture parts that require wire EDM, the team outsourced the manufacturing of this part to Machine Craft II Incorporated. While the cost of outsourcing complicated manufacturing tasks like this was relevant, the time spent and monetary cost of producing this part in-house would have been significantly greater than getting the part made by a third party.

Another complicated component within the design of the first iteration was a 6061-aluminum wedge that mounted to the front of the compliant mechanism and was designed to accept the entirety of the applied load from oncoming hypersonic flow, and the applied load from the pulsed laser. This component was manufactured using aluminum because of its high machinability, cost, weight, and because of the LLE's interest in aluminum as a material to test on with pulsed lasers. Because this component was significantly less complicated compared to the compliant mechanism, it could be manufactured using resources internal to the University of Rochester in a reasonable amount of time with 3-axis CNC milling.

Other parts manufactured for the first iteration sting include a collimator mount positioner, and the two housing halves for the compliant mechanism. The collimator mount positioner was machined out of 6061 aluminum because it needed to be stiff enough to maintain optical alignments when the system was taken apart and reassembled, and because tighter tolerances could be attained with a 3-axis mill as opposed to a FDM 3D printer. The two identical halves of the stings housing were manufactured using a Stratasys F270 FDM printer for its high accuracy and high strength thermoplastic printing capabilities. These two components were not manufactured out of metallic materials because they were not designed to carry significant loads, and because they are intricate parts that would require a significant amount of time to manufacture out of milled aluminum or steel.

The manufacturing methods for the second iteration of the sting were influenced by similar constraints that were present with the first iteration of the sting, except for the added time constraint. The development for the second iteration of the sting occurred a significantly accelerated schedule. The converged design leveraged manufacturing techniques that allowed us to get from

design and analysis to testing as fast as possible. The first part, the adapter flange, was a simple 1018 milled cylinder that was designed to interface with the sting mounting system in CUBRC's wind tunnel. The second part, the cantilever beam, was also manufactured out of 1018 steel rectangular bar stock because both parts needed to be welded together and 1018 is a relatively forgiving material when it comes to welding due to its low carbon content

While this system is far from scalable at its current stage of development, there are still several changes to the design that could be introduced that would make the system much more effective when being manufactured at high volume. For example, because the process of FDM 3D Printing is relatively slow, the housing pieces could be injection molded, a process much more suitable for plastic parts in high volume. Additionally, if the design of the sting was simply smaller than its current displacement, there would be significant cost savings not only from materials, but from machining time. The EDM process specifically took up the majority of the machining time for the third-party manufacturer and cutting down on the size of the system would significantly improve the ability to make many systems consecutively.

TABLE 4
SIGNIFICANT MANUFACTURING TASK HOURS AND COSTS

Part	Quantity	Labor (hrs)	Material/Hardware Cost ($)	Total ($)
Sting V1				
Core	2	0	0[2]	569.81
Wedge	1	6	31.84	631.84
Collimator mount	1	2	3.00	203.00
Housing	1	1	12.11	112.11
Sting V2				
Adapter mount	1	2	23.19	123.19
Cantilever Beam	2	1	5.70	105.70
			Total:	1,745.65

TABLE 5
TOTAL PROJECT DEVELOPMENT TIME

Member	Development Time
Asa Guldbrandsen	134.0 hrs
Maxwell Gjevre	90.2 hrs
Luke Herter	101.0 hrs
Alexander Lee	91.0 hrs
Miles Owens	121.5 hrs
Total Hours	537.7 hrs
Total Cost @ $100/hr	$53,770

[2] Material and labor costs were included in the quote for the two sting cores from Machine Craft Inc. II

TEST PLAN AND RESULTS

A crucial part of this project is testing and validation of the system being developed. Before any hypersonic testing could be performed, researchers had to first demonstrate that shock delivered by a pulsed laser could be resolved and analyzed in a laboratory setting.

The first specification, a minimum factor of safety of 10 for the mount, was verified by a bolt analysis of the mount. This specification was met for both design iterations as shown in the mechanical analysis. The second specification, data collection in at least one degree, was tested via calibration with the impulse hammer. It was found that a vertical force applied by the impulse hammer could be resolved in both design iterations. Specification three, a minimum sampling rate of 300 kS/s, was met due to the use of the GEN3i data acquisition system from Hottinger Brüel & Kjær (HBK) in both design iterations. The GEN3i system samples at a maximum of 500 kS/s. The DAQ was configured using the following specifications:

TABLE 6
HBK DAQ AND GAUGE SPECIFICATIONS

Gain	1 K
Bridge Factor	1
Gauge Factor	2.09
Excitation Range	+/- 1.5 V
Impedance	10 MΩ
Filter Frequency High	5 KhZ
Sampling Rate	500 kS/s
Strain Gauge Resistance	120Ω
Gauge Length	0.120"
Strain Range	+/- 3%
Matrix Size	0.62 X 0.42"

The fourth specification, a minimum resolved laser load of 0.2 lb_f, was tested in NX and at the LLE using an impulse hammer. LLE testing data for iteration two is shown in Figure 2. The first design iteration did not pass this specification, but the second design iteration did. As shown in the figure, there is a clear difference in strain that follows a somewhat linear fit as expected for iteration two. Specification four was originally a maximum laser load of 2000 lb_f, which was found to be far too high due to the time scale of the laser shot.

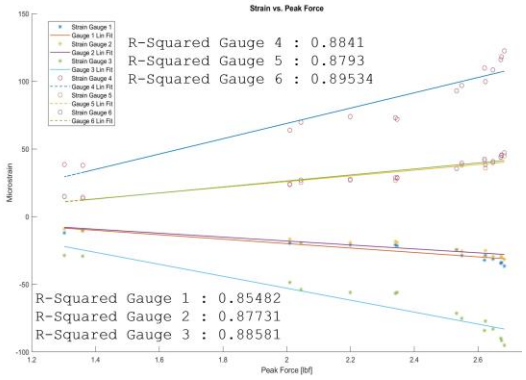

Figure 2: Iteration two calibration data plot and R-Squared values.

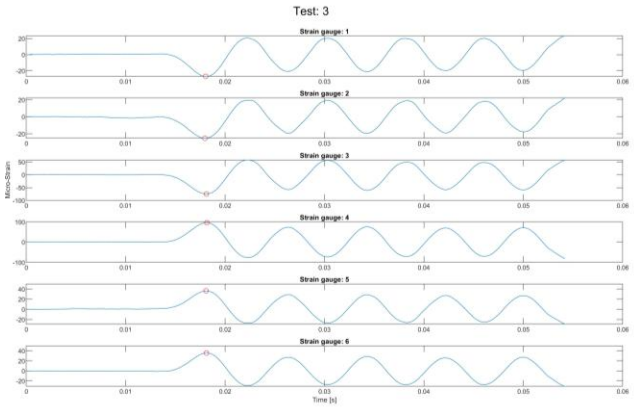

Figure 3: Iteration two example response from impulse hammer.

The test data shown in Figure 2 was collected by striking the face of the second iteration wedge with an impulse hammer and recording the voltage output of both the impulse hammer and strain gauges (Figure 3). This data was then analyzed using MATLAB to calculate the peak force, impulse, strain value, and R^2 value for each test. A total of 17 data sets were collected and analyzed for this calibration. A similar calibration was conducted for iteration one. Due to the increased stiffness of iteration one, it was unable to resolve a 0.2 lb_f load.

The fifth specification, a minimum acceptable flow load of 500 lb_f, was tested in NX. This specification was originally set to a maximum flow load of 5000 lb_f, which was found to be significantly higher than needed for the flow conditions at CUBRC. This specification was not approved by the sponsor. NX simulations suggest that this specification has been met, but without a physical test, this specification was not met. The sixth specification, a maximum build envelope of a 1 ft^3 cube, was verified in NX and was met for both iterations. The seventh specification, a maximum flow diameter of 48 in, was verified in NX and was met for both iterations. The eighth specification, a minimum natural frequency of 1 kHz, was computed in NX and was not met for either iteration.

TABLE 7
REVISED SPECIFICATIONS, PASS/FAIL

	Value	Specification	V.1 Pass?	V.2 Pass?
1	10 FoS	Minimum factor of safety for mount	Y	Y
2	1 DoF	Minimum data collection axis	Y	Y
3	300 kS/s	Minimum sampling rate	Y	Y
4	0.2 lb_f	Minimum load from impulse hammer	N	Y
5	500 lb_f	Minimum flow load	N	N
6	1 ft^3	Maximum size	Y	Y
7	48 in	Maximum flow diameter	Y	Y
8	1 kHz	Minimum natural frequency	N	N

The first requirement, no mechanical failure due to hypersonic flow, was validated using NX. Simulations suggest that the prototype would not fail, but without hypersonic testing this requirement cannot be verified. The second requirement, compatibility with diagnostics currently used by the LLE, was met for both iterations. The third requirement, resolution of a pulsed laser impulse, was tested at the LLE using a focused laser that could deliver approximately 2.2 Joules of energy to the sting. This requirement was added because the team found that this task was more difficult than expected. This requirement was not met in either case. Figure 4 shows a laser shot test on the first iteration. As can be seen, there is no obvious response, and the data is essentially all noise.

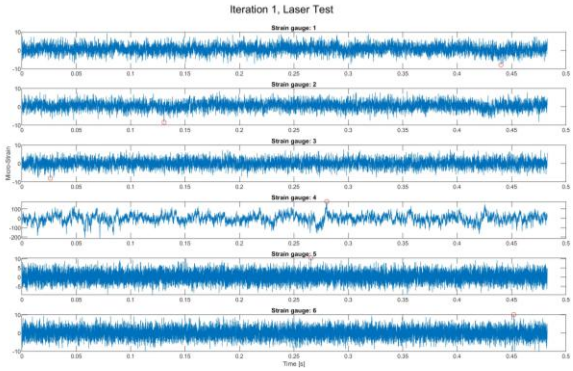

Figure 4: Noise recorded during laser testing with iteration one.

Requirement three represents the area with the most room for improvement. Multiple laser shots were performed on both versions of the prototype, and neither were able to resolve any meaningful data, as shown above. In an effort to better understand the load applied by the laser, the team tried shooting a simple cantilever beam and were able to see an electrical response, but the testing did not yield expected results. As shown in Figure A23A, the strain gauges provided an electrical response in the form of a jump in voltage, recorded as a jump in strain. It is unclear the exact meaning of this jump, but in any case, the pulsed laser shot results in a change in resistance in the gauge. Future work would include replication of this testing to better

understand the capabilities of strain gauges for impulse laser data collection.

TABLE 8
REVISED REQUIREMENTS, PASS/FAIL

	Requirement	V.1 Pass?	V.2 Pass?
1	Must not mechanically fail when subject to hypersonic flow	N	N
2	Must be compatible with the diagnostics known to the LLE group	Y	Y
3	Must be able to resolve impulse load applied via pulsed laser	N	N

Throughout the design process, it was found that the initial understanding of hypersonic flow and pulsed laser effects was flawed and required more analysis before determining requirements and specifications.

Additionally, the original testing plan included interferometry as a key component of the data acquisition system. Although this method was ultimately removed from the final experimental setup due to power supply issues, it remains a highly viable technique for future work and should be strongly considered in subsequent investigations. Interferometry offers exceptional displacement resolution, making it particularly well suited for measuring the extremely small deflections expected in impulse-laser and hypersonic applications.

The interferometric testing procedure began with the precise alignment of the helium-neon (HeNe) laser and the collimator. Because efficient coupling into the fiber-optic system requires near-perfect alignment, a series of fine angular and translational adjustments were performed. Once alignment was achieved, the stationary reference mirror was positioned outside the wind tunnel, while the measurement mirror was mounted on the test article inside the device. The recombined output beam was then projected onto a Phantom high-speed camera for real-time recording and analysis.

Interferometry operates by comparing the phase of two coherent light beams. One beam reflects from the fixed reference mirror, while the other reflects from the moving measurement surface. When these beams recombine at the coupler, they interfere constructively or destructively depending on their relative phase difference. Constructive interference occurs when the wave peaks align, producing a bright fringe, while destructive interference occurs when a peak aligns with a trough, producing a dark fringe.

As the test article displaces, the optical path length of the measurement beam changes. This alters the phase relationship between the two beams, causing the interference fringes to shift across the output image. By tracking this fringe movement, extremely small displacements can be quantified. Since the wavelength of the HeNe laser is approximately 632.8 nm, each full fringe shift corresponds to a path-length change of one wavelength. For reflective measurements, this translates to a physical surface displacement of one-half wavelength, or approximately 316 nm. This extraordinary sensitivity is what makes interferometry such a powerful tool for precision displacement measurements.

INTELLECTUAL PROPERTY

The current design appears to be patentable, as there have been no existing patents that closely resemble it. While there are current patents for a force measurement system for a hypersonic wind tunnel [1], that design incorporates embedded data acquisition systems within the sting itself and differs significantly from ours.

In addition, the patented design relies on an elastomeric material that deforms under load and then returns to its original shape. In contrast, our design uses steel as the primary structural material. Deformation is measured using strain gauges, a phantom camera, and interferometry, rather than through embedded sensing systems. These substantial differences in both material selection and measurement methodology distinguish our design from existing patented technologies.

SOCIETAL AND ENVIRONMENTAL IMPLICATIONS

These prototypes have the potential to advance research in hypersonics and improve data acquisition techniques for impulse laser facilities. By investigating how impulse lasers affect strain gauge measurements, this work will provide valuable insight into the feasibility and reliability of using strain gauges in hypersonic flow environments. This will enable future researchers to confidently implement strain gauges in similar applications and more accurately interpret the data they collect.

At present, the practical applications of impulse laser effects on objects traveling at hypersonic speeds are relatively limited. Many of the most promising concepts are in the aerospace and extraterrestrial domains. For example, a spacecraft or spacecraft could potentially use directed laser energy to alter the trajectory of small objects or debris in space, helping to avoid collisions or reroute hazards.

Beyond these futuristic applications, impulse laser technology also has important implications for laser ablation more broadly. Laser ablation is already widely used in precision manufacturing, particularly in industries that require extremely fine material removal. For instance, semiconductor manufacturers rely on laser processes to create intricate features and remove material during the fabrication of silicon chips. These existing applications highlight the broader potential of advancing impulse laser technologies.

From an environmental perspective, the equipment used in this project is composed of standard materials and systems that are generally safe for the environment. However, the experimental process consumes a large amount of energy, with each test shot requiring significant amounts of energy to operate the wind tunnel and all the auxiliary control and measurement systems connected to it. While this level of energy consumption may raise concerns about efficiency, it is important to recognize that such demands are typical for advanced hypersonic research facilities. As technology continues to evolve, the efficiency of both the experimental process and the supporting equipment is expected to improve, enabling more tests at lower monetary and environmental costs.

RECOMMENDATIONS FOR FUTURE WORK

Given extra time, the group would go through another design cycle using the new understanding of loading conditions, shock behavior, and the capabilities of strain gauges. A potential concept design using thin spring steel webs to further increase displacement is shown in Figures A12, A13. There are concerns, however, that a highly compliant system would be prone to extreme deformation or buckling when subjected to hypersonic flow. Furthermore, the coupling of diagnostic systems that require very small deformations (interferometry, strain sensing) with systems that require large deformations (Schlieren imaging) will hinder all the measurement systems' ability to record the desired behaviors. This calls for designing either a system that utilizes diagnostics that measure entirely using large deformations (millimeter-scale), or entirely small deformations (micrometer-scale).

Despite the technical delays that prevented the group from using the fiber-optic interferometer for diagnostics, the system appeared to have promising performance characteristics. After discussing the operation of the actual wind tunnel with engineers at CUBRC, there are serious concerns such as high vibration and movement of the tunnel during testing which cannot be ignored when considering the effectiveness of the interferometer.

As far as diagnostics that this project did not cover, photon doppler velocimetry (PDV) appears to be very well-suited for indirectly measuring the impulse delivered by a pulsed laser. PDV systems can measure the high-speed movements of materials when they are subjected to shock, vibration, or other dynamic loading. In this case, the intensity of the shock generated by a pulsed laser could be correlated with the impulse required to create the shock. It is possible, though, that employing the PDV system to measure force would also be subject to the same limitations of a Michelson interferometer like the one the Hyper group developed as it is also an optical measurement technique.

ACKNOWLEDGMENTS

The Hyper group would like to thank Ben Martin, Valerie Fleischauer, Vincent Tagliamonti, Jerry Chung, Riley Flaum, Chris Pratt, Jim Alkins, Bill Mildenberger, Sam Kriegsman, Edward Herger, Chris Muir, Kyle Christensen, Elizabeth Martin, and HBK for their support.

REFERENCES

[1] Y. Zhang, X. Liu, J. Wang, and Z. Li, "Hypersonic vehicle force measurement sting with built-in signal acquisition system," China Patent CN111122104B, Jul. 15, 2022. CN111122104B - Plane symmetry hypersonic aircraft hood separation wind tunnel test device - Google Patents

[2] Defense Technical Information Center (DTIC), 1997, "Large Energy National Shock Tunnel (LENS) Description and Capabilities," ADA338839, https://apps.dtic.mil/sti/pdfs/ADA338839.pdf

[3] Vishay Measurements Group, Inc., 1992, *Student Manual for Strain Gage Technology*, Bulletin 309E, Vishay Intertechnology, Inc., https://intertechnology.com/Vishay/pdfs/StudentGuideManual.pdf

[4] Micro-Measurements (Vishay Precision Group, Inc.), n.d., *Strain Gage Sensor Reference Guide* (Document ID 8690), https://docs.micro-measurements.com/?id=8690

[5] Aerolab LLC, n.d., "Sting Balance," Aerolab, https://www.aerolab.com/aerolab-products/sting-balance/

[6] FUTEK Advanced Sensor Technology, Inc., n.d., "Wind Tunnel Sensing," *FUTEK*, https://www.futek.com/applications/wind-tunnel-testing

[7] Li, S., Liu, Z., Zhao, F., and Gao, H., 2022, "A New Hypersonic Wind Tunnel Force Measurement System to Reduce Additional Bending Moment and Avoid Time-Varying Stiffness," *Sensors*, 22, p. 2572. https://doi.org/10.3390/s22072572

[8] National Aeronautics and Space Administration (NASA), 2012, "Wind-Tunnel Balance Characterization for Hypersonic Research Applications," NASA Technical Report, https://ntrs.nasa.gov/api/citations/20120006725/downloads/20120006725.pdf

[9] Defense Technical Information Center (DTIC), 1976, "Sting Dynamics of Wind Tunnel Models," ADA024445, https://apps.dtic.mil/sti/tr/pdf/ADA024445.pdf

[10] Defense Technical Information Center (DTIC), 1965, “A Low-Load Three-Component Force Balance for Measurements in.a Low-Density Wind Tunnel,” AD0453130, https://apps.dtic.mil/sti/tr/pdf/AD0453130.pdf

[11] Defense Technical Information Center (DTIC), 1994, “Hypersonic Wind Tunnel Test Techniques,” ADA284057, https://apps.dtic.mil/sti/tr/pdf/ADA284057.pdf

APPENDIX A: TABLES

TABLE A1
ORIGINAL REQUIREMENTS AND SPECIFICATIONS

Specifications	# Value	Units	description
1	10	FoS	All parts must have a simulated factor of safety higher than this value prior to physical tunnel tests.
2	1	Dof	Device Must collect data in at least this number of degrees of freedom.
3	300	kHz	Device must collect data at a rate of at least this value.
4	2000	lbf	Upper limit of the vertical force that the apparatus can accept
5	5000	lbf	Axial force range that the apparatus can accept (Force applied by aerodynamic force)
6	1	ft3	All sting balance components must fall into a cube-shaped volume of this size.
7	48	in	The sting support structure must be designed to accommodate a circular flow regime with this diameter.
8	10	C	Temperature change that the device must be designed to accept without losening bolts, or major change to vibrational modes. (-5 -+10)
9	1	kHz	Lowest natural frequency of the apparatus
		Requirements	**description**
		1	Must be designed to not fail when subjected to hypersonic flow
		2	Must be compatible with other known diagnostics used by the PLE group

TABLE A2
WORK BREAKDOWN STRUCTURE

			$/hr		cost	Hrs				
T	P1 - Tech		$ 100.00		$ 8,450.00	84.5				
D	P2 - Design Eng.		$ 150.00		$ 20,887.50	139.25				
A	P3 - Analyst		$ 200.00		$ 15,200.00	76		Total Cost		
M	P4 - Machinist		$ 75.00		$ 2,250.00	30		$ 46,787.50		
						329.75				
	Phase	Item		Date	Activity	Time (hr)	Skill	Cost	Task	Start
Start				2/5	Start	0			Start	
a0	Design/Simulation						D	$ -	a0	
a1		Research sensors, load cases (flutter, drag forces, LAF)			research	40	D	$ 6,000.00	a1	
a2		Decide methods			decide-methods	15	D	$ 2,250.00	a2	
a3		Hand Calculations			hand-calcs	10	D	$ 1,500.00	a3	
a4		Design Wedge			design-wedge	1	D	$ 150.00	a4	
a5		Design Sting Balance			design-sting	15	D	$ 2,250.00	a5	
a6		Design Support structure/Base			design-mount	15	D	$ 2,250.00	a6	
a7		Interferometry system design			interferometry-design	20	D	$ 3,000.00	a7	
a8		Method 2 system design			force-design	20	D	$ 3,000.00	a8	
a9		Full sting FEA			FEA	30	A	$ 6,000.00	a9	
a10		Full sting Modal analysis			modal_analysis	30	A	$ 6,000.00	a10	
b0	Prototype								b0	
b1		3D Printed 1st Iteration		20-Feb	3d-print	4	T	$ 400.00	b1	
b2	Order:	All supplies/hardware for interferometry			interferometry-hardware	1	D	$ 150.00	b2	
b3		All supplies/hardware for method 2			force-hardware	1	D	$ 150.00	b3	
b4		Sting, sting support, base, and other stock materials			SMC	1	D	$ 150.00	b4	
b5		Order purchased parts (bolts, centering rings)			purchase from mmc	0.25	D	$ 37.50	b5	
b6	Machining	Machine Sting			make-sting	13	M	$ 975.00	b6	
b7		Machine Sting Support Structure and base			make-mount	10	M	$ 750.00	b7	
b8		Machine Wedges			make-wedge	7	M	$ 525.00	b8	
b9	Assemble	Put it all together			assembly	2	T	$ 200.00	b9	
c0	Test Preparation								c0	
c1		Calibrate Data acquisition using impulse hammer		20-Mar	calibrate	15	T	$ 1,500.00	c1	
c2		**Call the ball**		27-Mar	ctb	0	D	$ -	c2	
c3		Laser Shot testing			laser-testing	24	T	$ 2,400.00	c3	
c4		Develop program for postprocessing tunnel data			code	15	T	$ 1,500.00	c4	
d0	Test Data								d0	
d1		Secure testing date		17-Mar	schedule-date	0.5	T	$ 50.00	d1	
d2		Onsite tunnel testing		17-Apr	real-test	24	T	$ 2,400.00	d2	
d3		Postprocess data			postprocess	8	A	$ 1,600.00	d3	
d4		Write up		1-May	report	8	A	$ 1,600.00	d4	
End		End		1-May	End				End	

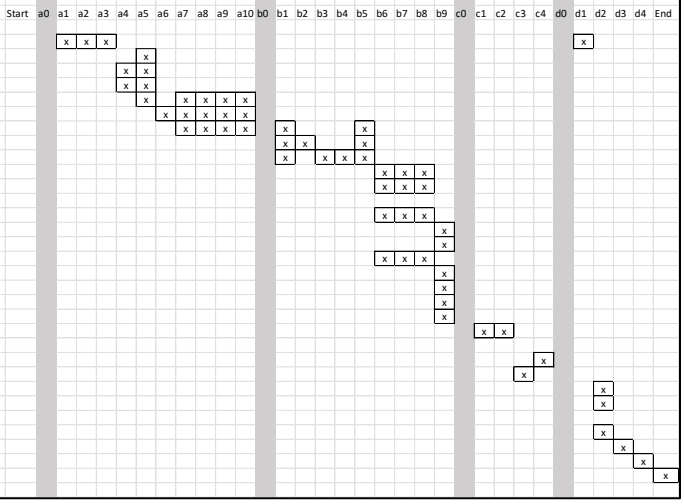

TABLE A3
PUGH MATRIX DESCRIBING THE MEASUREMENT SELECTION PROCESS

	Phantom Camera	Purchased Interferometer	Custom Interferometer	LK-G Sensor	Strain Gages
Lead Time	0	-	0	0	0
Ease of Use	0	0	--	-	+
Vacuum	0	0	0	--	0
Sampling Rate	0	+	+	-	---
Cost	0	--	0	0	0
Total	0	-2	-1	-4	0

TABLE A4
ITERATION TWO, CANTILEVER BEAM ANALYSIS RESULTS

6" CBEAM [1" x thickness] SOL129 Al 6061 (NX) "Wedge"	Max. Stress (psi)	thickness (in)		
		0.3	0.4	0.5
load (lbf)	24.5	14580.00	10363.61	6801.10
	25.0	14870.00	10575.11	6939.90
	50.0	29750.00	21150.00	13880.00
	100.0	59480.00	42300.00	27750.00

	Max. Disp (in.)	thickness (in)		
		0.3	0.4	0.5
load (lbf)	24.5	0.09	0.0479	0.028
	25.0	0.0914	0.0489	0.0286
	50.0	0.183	0.098	0.0571
	100.0	0.366	0.196	0.114

APPENDIX B: FIGURES

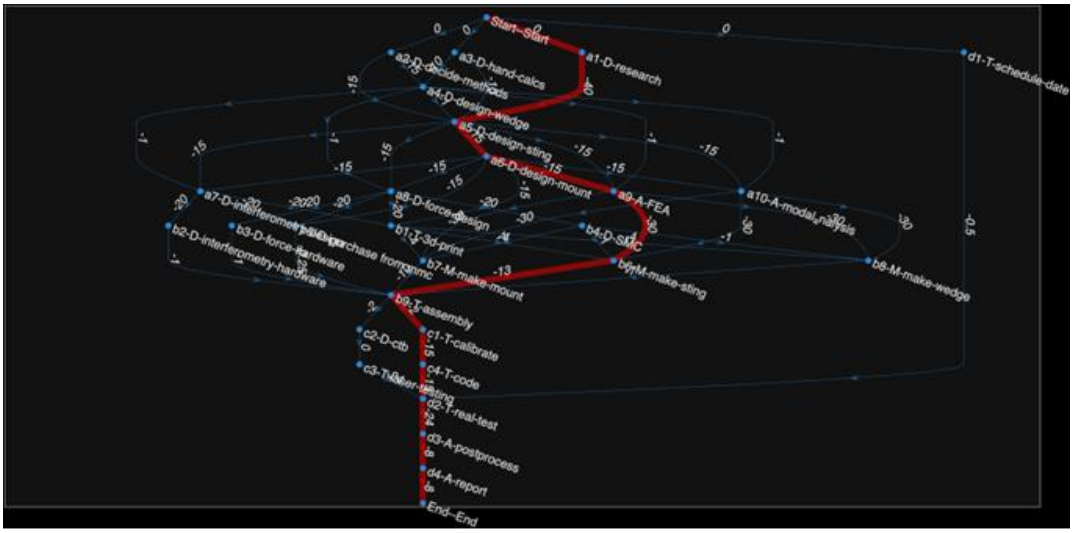

Figure A1: MATLAB-generated flowchart showing the critical path.

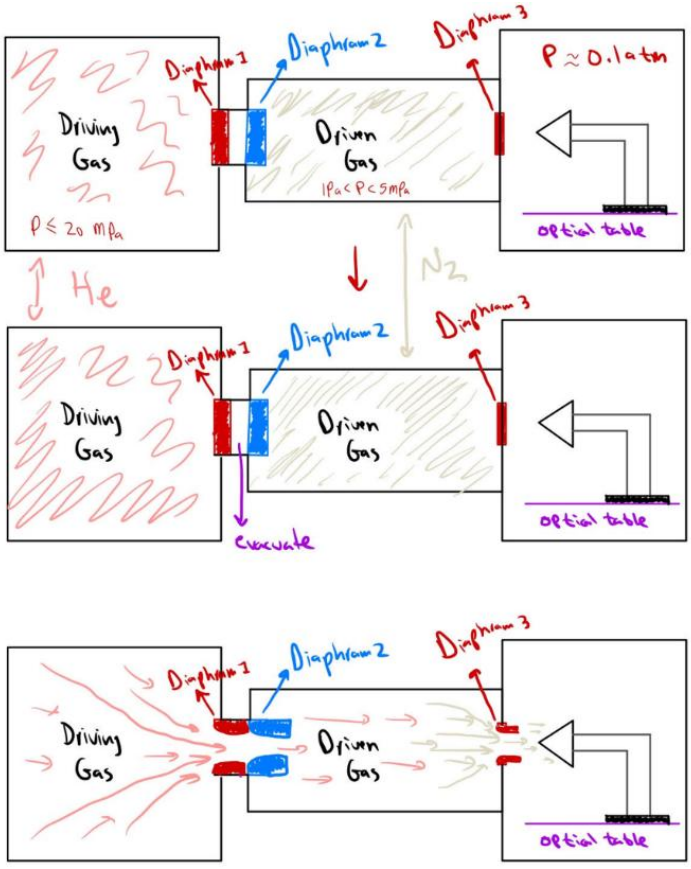

Figure A2: Basic sketch of the tunnel operation.

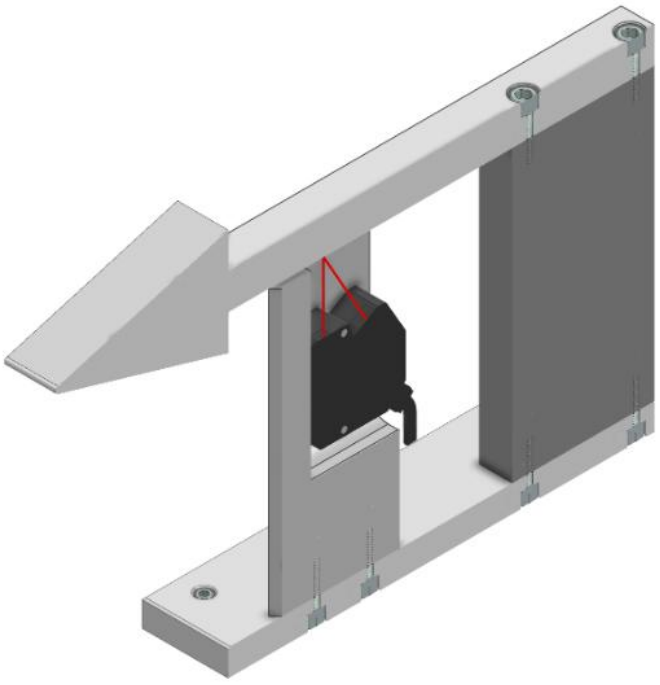

Figure A3: Sting design using an LK-G5000 sensor, with a wedge to keep out of direct flow.

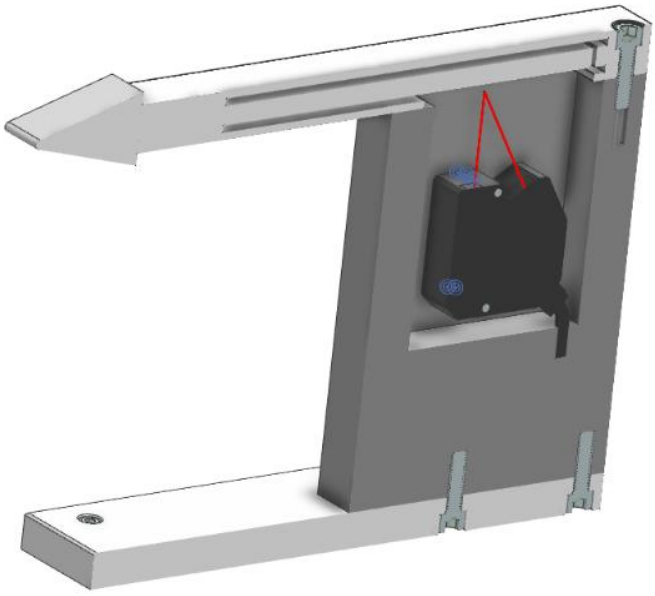

Figure A4: Sting design with the LK-G5000 sensor in a fully-enclosed chamber.

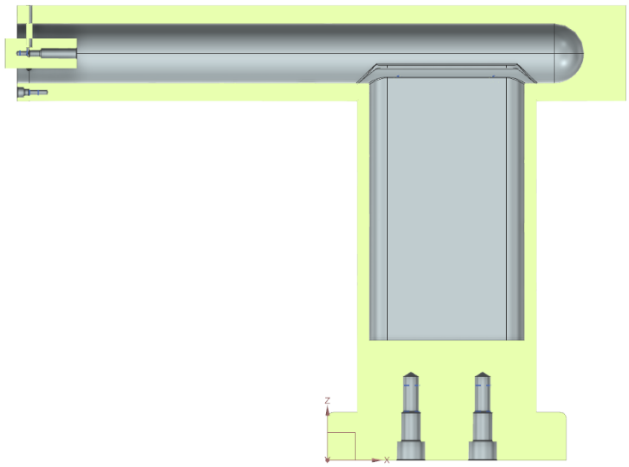

Figure A5: Sting design with a hollow section to allow wires and measuring devices to sit outside of flow. At the far left there is a compliant mechanism allowing for controlled movement.

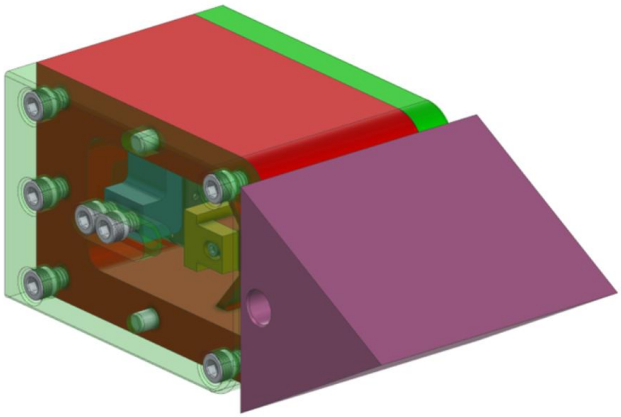

Figure A6: First concept sting design with compliant mechanism and revised optical mounting.

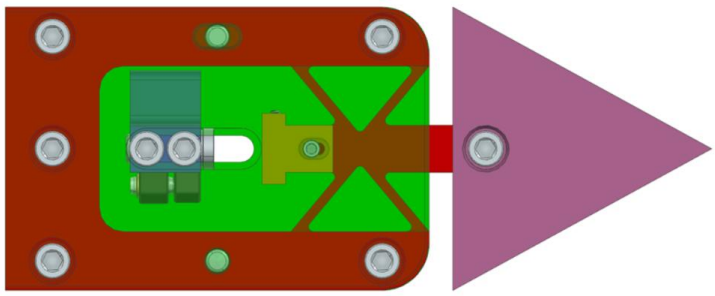

Figure A7: First iteration concept sting design with compliant mechanism and revised optical mounting.

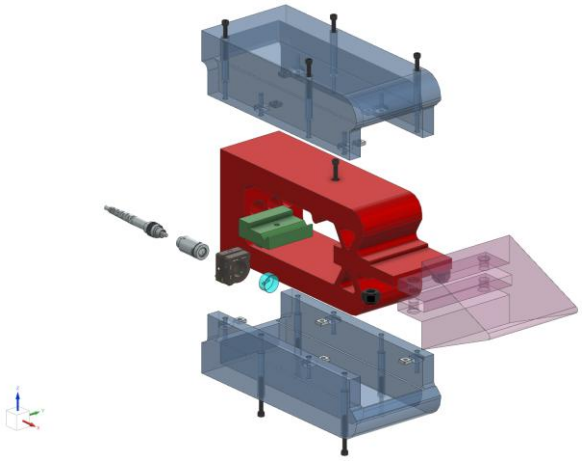

Figure A8: Finalized iteration one design.

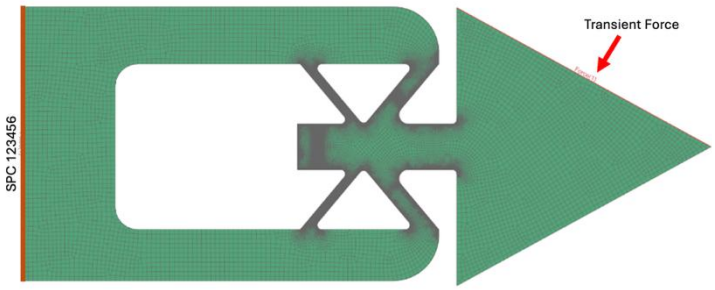

Figure A9A: FEM Mesh with applied constraint and force

Iteration	Mesh Size (in)	Max Stress (psi)	%Change
1	0.0010	7.01E+04	N/A
2	0.0005	7.37E+04	5%
3	0.0003	7.66E+04	4%
4	0.0003	7.76E+04	1%
5	0.0002		
6	0.0002		

Figure A9B: Convergence study to determine mesh size.

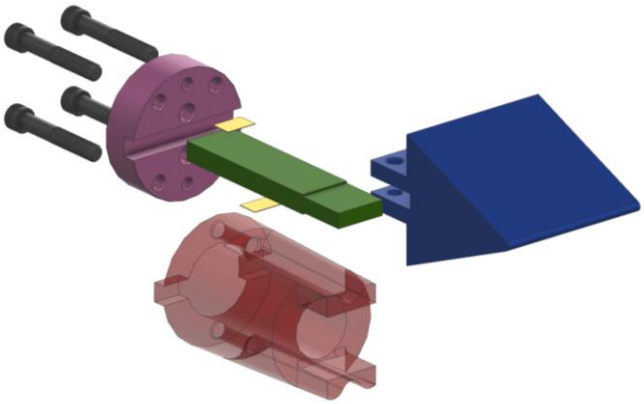

Figure A10: Finalized iteration two design.

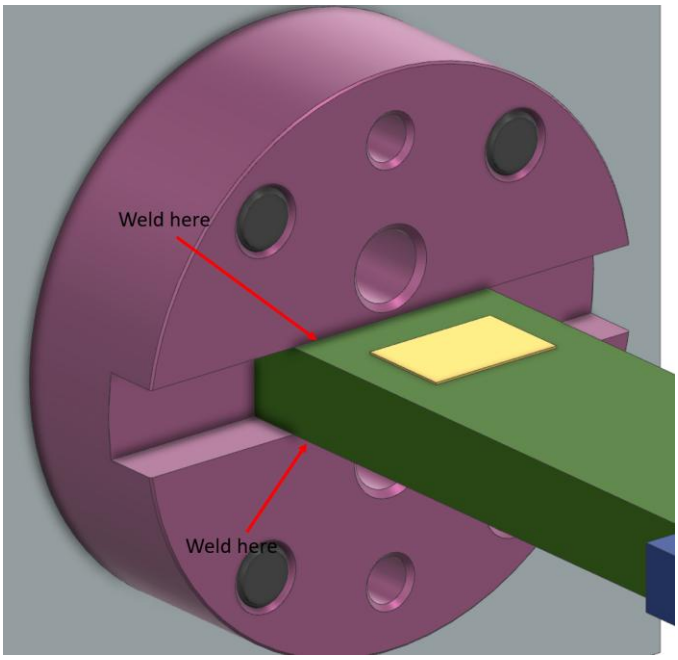

Figure A11: Iteration two weld location.

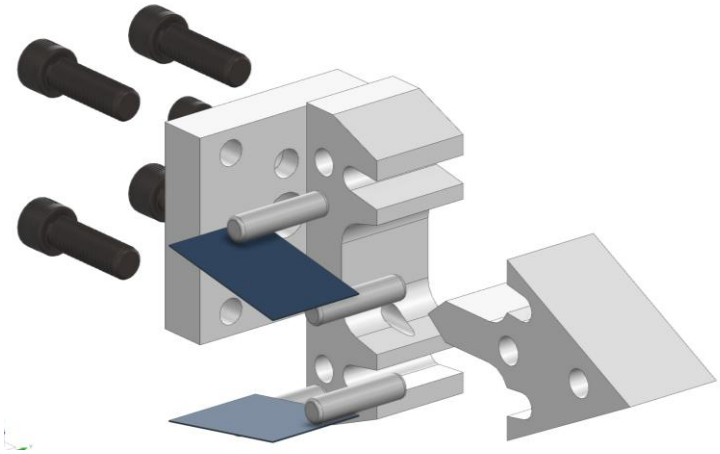

Figure A12: Concept iteration three design, exploded.

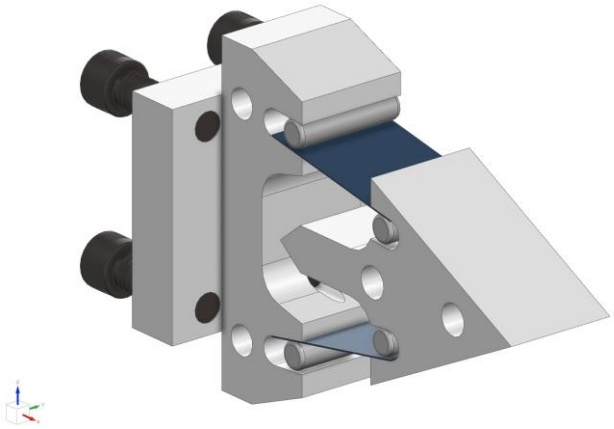

Figure A13: Concept iteration three design, assembled.

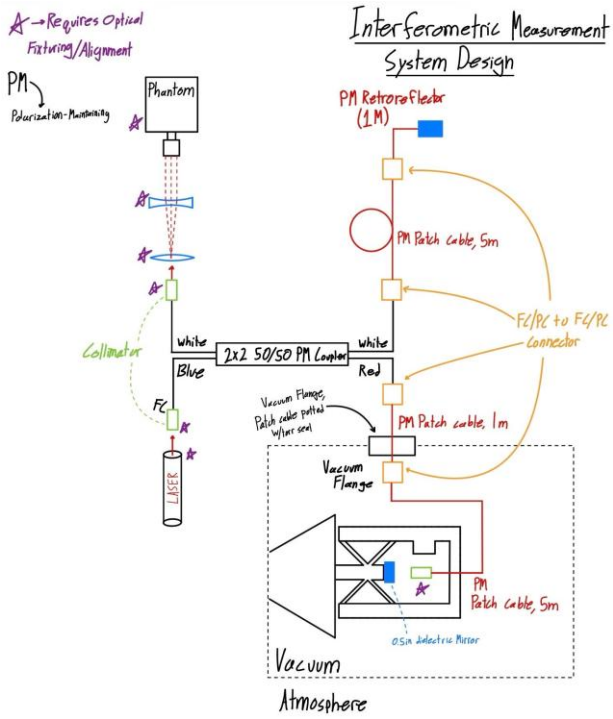

Figure A14: Interferometric system design.

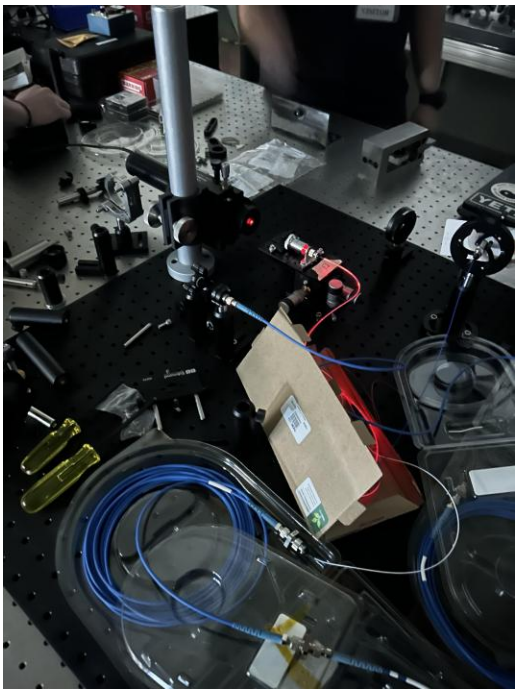

Figure A15: Initial setup of fiber-optic interferometer.

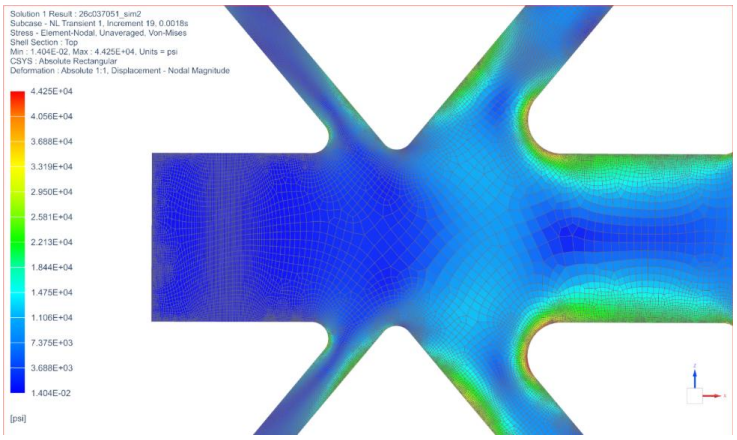

Figure A16: Simulated Von Mises stress distribution in webbing of mechanism.

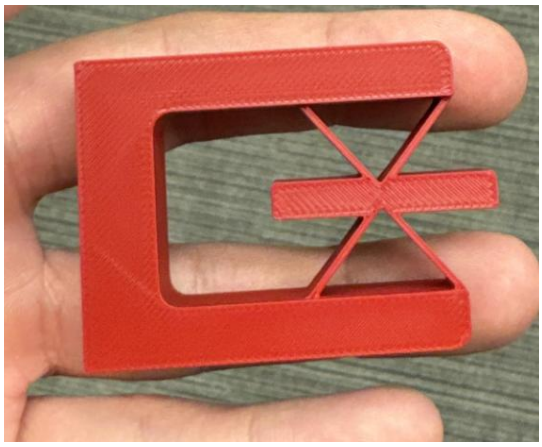

Figure A17: Initial 3D printed model of the mechanism.

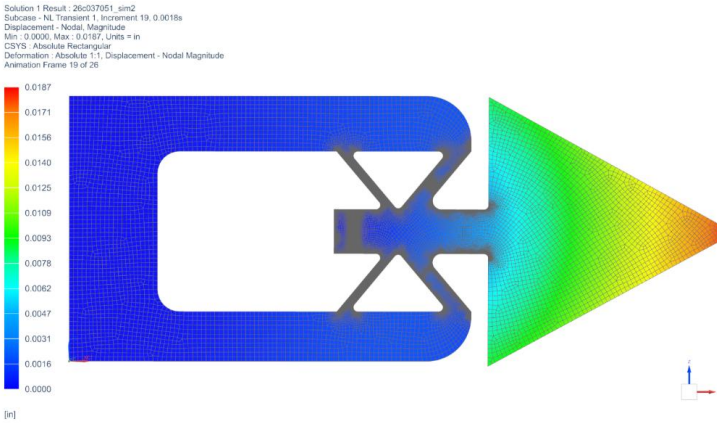

Figure A18: Maximum simulated displacement for flexible design.

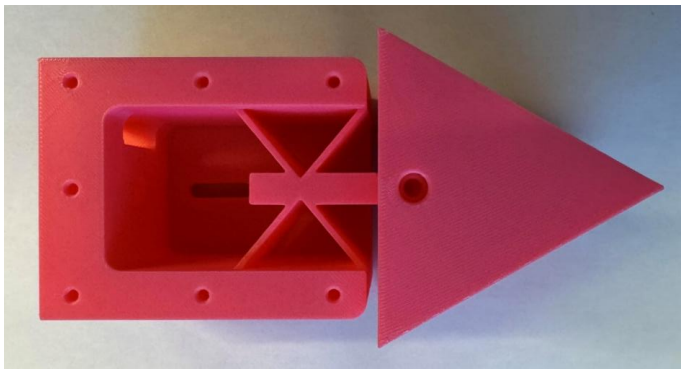

Figure A19: Frankenstein model.

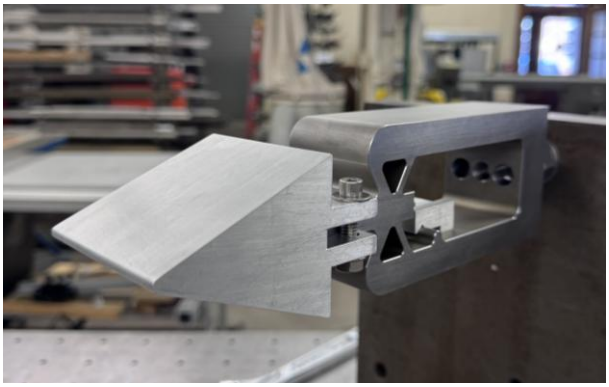

Figure A20: Assembled sting, first iteration without strain gauges.

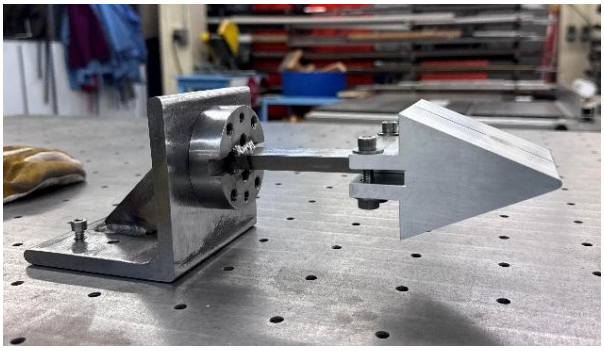

Figure A21: Assembled Sting, second iteration without strain gauges.

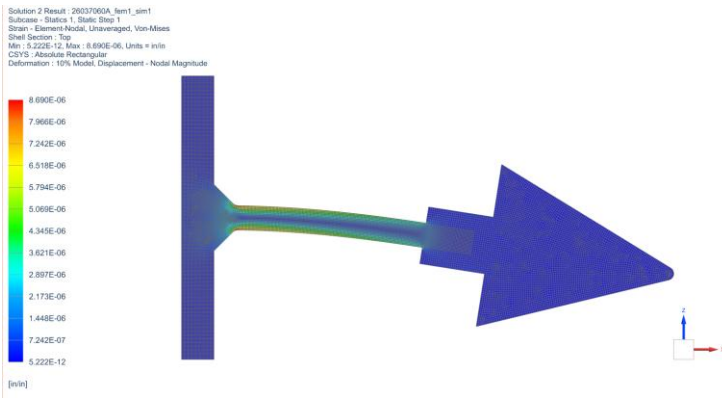

Figure A22: Cantilever beam stress results.

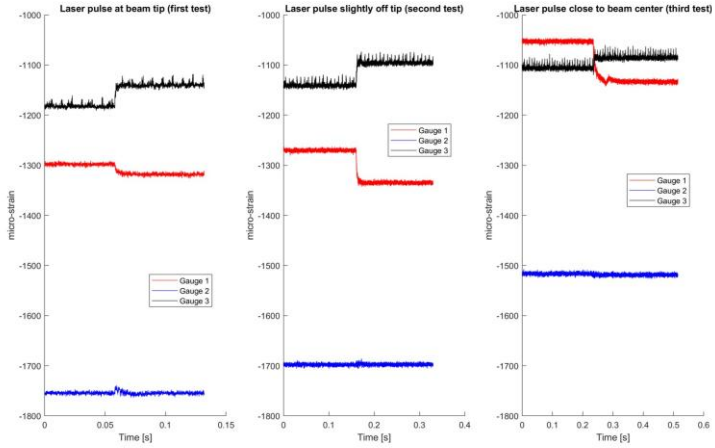

Figure A23A: Strain gauge data of aluminum bar.

Gauges	Pulse at tip	Pulse off tip	Pulse near middle	Units
"One"	20.24	64.542	71.593	"micro-strain"
"Two"	0.38162	-0.34598	2.0933	"micro-strain"
"Three"	-42.28	-45.207	-18.58	"micro-strain"

Figure A23B: MATLAB output for aluminum beam laser shot testing.

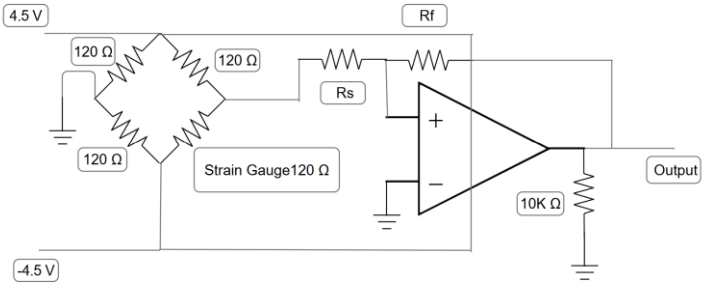

Figure A24: Circuit diagram of a single Wheatstone bridge coupled with a 220-gain amplifier.

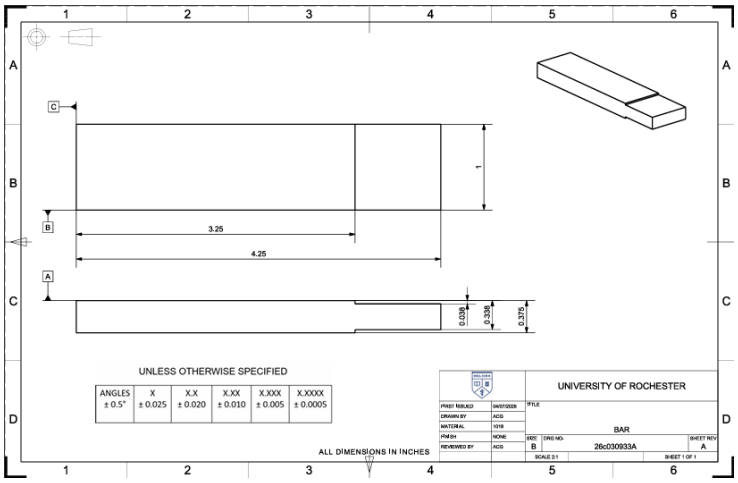

Figure A25: Drawing of the bar for the second iteration.

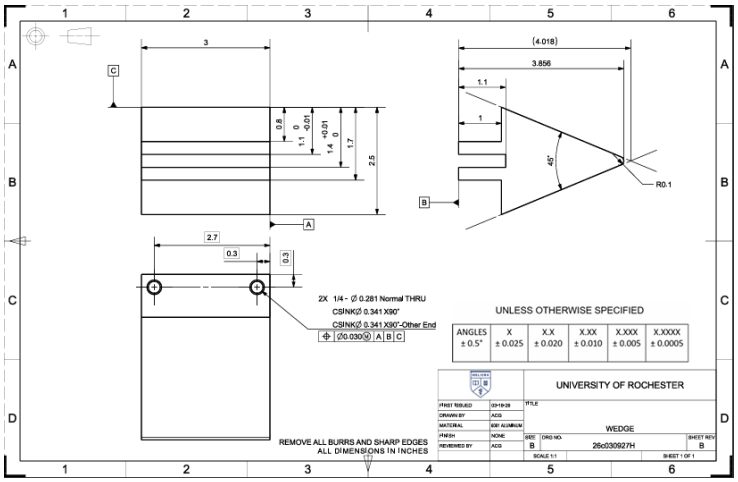

Figure A26: Drawing of the wedge used across both iterations.

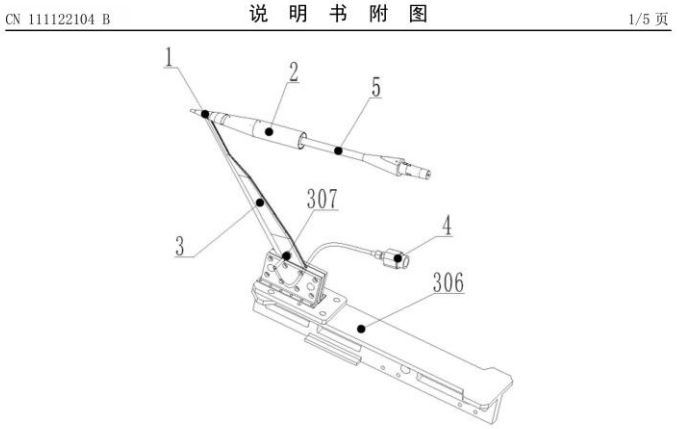

Figure A27: Patent search results for a hypersonic sting.

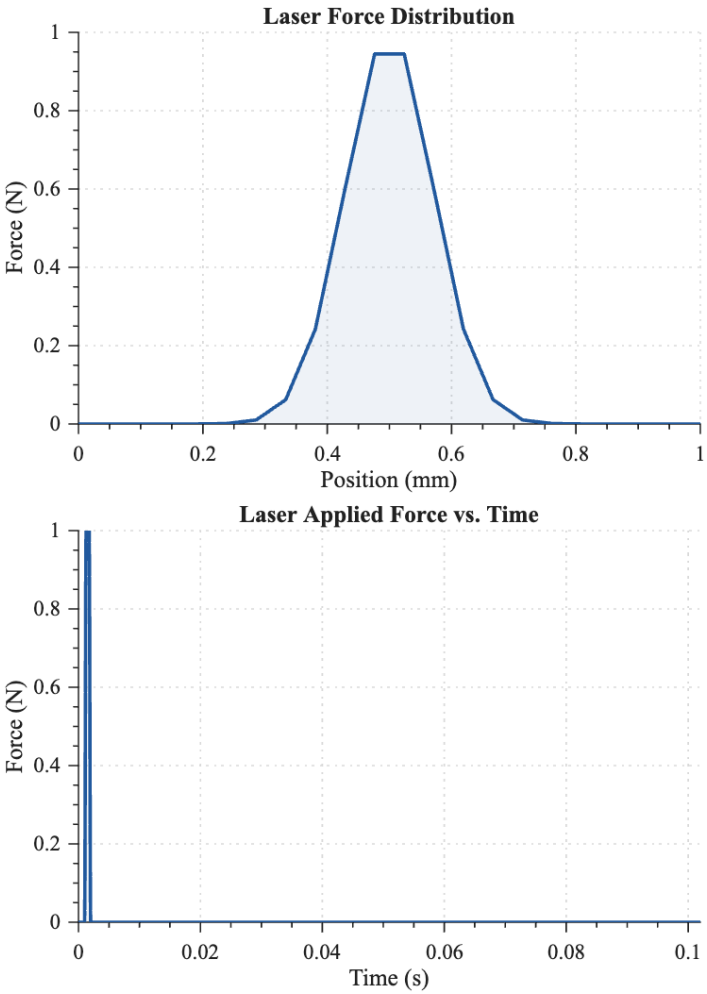

Figure A28: Spatial and Temporal Force Distributions used for all FEA modeling.

APPENDIX C: EQUATIONS

Newton's Sine-Squared Law:

$$C_p = 2sin^2(\theta) \tag{1}$$

The pressure coefficient for flow where M>>1, where θ is deflection angle.

Pressure:

$$P = C_p \frac{1}{2}\rho V^2 \tag{2}$$

C_p is the pressure coefficient, ρ is air density, and V is the velocity of flow.

Force:

$$F_t = PA \tag{3}$$

P is the pressure on the wedge face and A is the frontal area of the system.

Bolt Torque-Preload Relation:

$$T = KdF_i \tag{4}$$

K is the torque coefficient, d is the major diameter, and F_i is the preload force.

Preload Force:

$$F_i = 0.75A_tS_p \tag{5}$$

S_p is the proof strength of the bolt material and A_t is the tensile stress area.

Endurance Strength:

$$S_e = K_aK_bK_cK_dK_eK_f\frac{S_{ult}}{2} \tag{6}$$

The $K_{a\text{-}f}$ values are unitless modification factors of surface condition, size, load, temperature, reliability, and miscellaneous-effects respectively, and S_{ult} is the ultimate strength.

Alternating Stress:

$$\sigma_a = \frac{F_{max} - F_{min}}{2A_t} \tag{7}$$

Mean Stress:

$$\sigma_m = \frac{F_{max} + F_{min}}{2A_t} \tag{8}$$

F_{max} and F_{min} are the maximum and minimum forces applied to the component, and A_t is the tensile stress area.

Modified Goodman Criterion:

$$\frac{\sigma_a}{S_e} + \frac{\sigma_m}{S_{ult}} \geq 1 \tag{9}$$

σ_m, σ_a, S_e, and S_{ult} are the mean stress, alternating stress, endurance strength, and ultimate strength respectively, and finite life is predicted when the left-hand side exceeds unity.